Global NEST Journal, Vol 20, No X, pp XX-XX

Investigation of adsorptive properties of Ag_2CO_3-polyaniline composite for environmental pollution control

Asadollahi A.[1], Ansari R.[2*] and Ostovar F.[3]
[1]Department of Chemistry, Faculty of Science, University of Guilan, P.O.Box 41635-1914, Rasht, Iran
[2]Department of Chemistry, Faculty of Science, University of Guilan, P.O.Box 41635-1914, Rasht, Iran
[3]The Environmental research institute, the Academic Center for Education, Culture & Research (ACECR), Rasht, Iran
Received: 27/06/2018, Accepted: 11/10/2018, Available online: 15/10/2018
*to whom all correspondence should be addressed: e-mail: ransari271@guilan.ac.ir
https://doi.org/10.30955/gnj.002808

Abstract

In this research, the Ag_2CO_3-PANI composite was synthesized with a simple precipitation method and then used as an effective adsorbent for adsorption of Methylene Blue cationic dyes from aqueous solution. Characterization of the adsorbent was carried out using UV–visible diffuse reflectance spectroscopy (UV–Vis DRS), X-ray diffraction (XRD), Fourier transform infrared spectroscopy (FT-IR) and scanning electron microscopy (SEM). The various parameters such as pH, contact time, sorbent dosage, initial dye concentration, and dye solution temperature were investigated. The optimum photo-catalytic activity of Ag_2CO_3-PANI at a weight content of 50% PANI for the degradation of MB was almost 86% that is much higher than the pure Ag_2CO_3 and PANI. The results showed an efficient removal at pH 10.0, within 60 min, and by using 1 g L^{-1} Ag_2CO_3-PANI composite at the temperature of 32˚C. The kinetic and equilibrium data fit into pseudo-second-order kinetic (R^2> 0.84) and Freundlich isotherm (R^2> 0.99) models, respectively. Adsorption capacity (q_0) calculated from Langmuir isotherm was found to be 55 mg/g. Thermodynamic studies indicated that the adsorption process was endothermic (ΔH°>0). The adsorption/desorption experiments were carried out attaining regenerations of up to 97% from MB, using distilled water and 0.1N HCl. The composite indicated high efficiency adsorptive properties and high reusability.

Keywords: Adsorption, Ag_2CO_3-PANI composite, adsorbent, methylene blue.

1. Background

Investigations show that more than 10,000 synthetic dyes are available annually at with over 7×10^5 ton. Many dye pollutants exhibit a high degree of sustainability against biological degradation and remain stable for a long time. These compounds and their derived products are poisonous or carcinogenic agents; they can cause a genetic mutation. Also, these the contaminations prevent the growth of bacteria that can destroy the impurities and causing an imbalance in the environment (Cheng *et al.,* 2014; Wang *et al.,* 2014a; Gupta *et al.,* 2015; Yao *et al.,* 2015). Many different methods, including biological treatment, coagulation/flocculation, membrane filtration, electrochemical methods, advanced oxidation processes and adsorption, have been used for the dye removal from water and wastewaters (Ai *et al.,* 2010; Mittal *et al.,* 2010; Ayad and El-Nasr, 2012; Saleh *et al.,* 2014; Yao *et al.,* 2015; Robati *et al.,* 2016). Among the various techniques for removal of dye, the adsorption method has been considered the most cost-effective method for environmental problems and it can remove classes of pollutants that are not easily degradable (Ahmaruzzaman and Gupta, 2011; Bao *et al.,* 2011; Gupta *et al.,* 2011; Gupta *et al.,* 2013; Xiong *et al.,* 2013; Yao and Liu, 2014). Photocatalytic degradation method has been applied for treatment of wastewater. This method has advantages such as low consumption of chemicals, no sludge production, relatively high mineralization, but by-products may be formed in this process (Crini, 2006; Yu *et al.,* 2014; Ghaedi *et al.,* 2015; Yu *et al.,* 2016; Saravanan *et al.,* 2013a; Saravanan *et al.,* 2016). Traditional semiconductors can only absorb the small amounts of photons in the visible region and need to irradiation of UV light for excitation, while sunlight irradiation is composed of 3-5% UV light and approximately 43% visible light. Moreover, the high recombination rate of the photo-excited electrons and holes are their drawback (Di-Paola *et al.,* 2012; McEvoy and Zhang, 2014; Wang *et al.,* 2010; Saravanan *et al.,* 2013b). Silver-containing compounds such as Ag_2CO_3 possess distinct advantages as photocatalyst due to SPR effect of metallic silver nanoparticles that are produced in visible light (Ai *et al.,* 2013; Dai *et al.,* 2014; Wang *et al.,* 2014b; Xu *et al.,* 2011; Xu *et al.,* 2015; Dai *et al.,* 2012). The formation of silver semiconductor and other compounds can produce heterojunctions that greatly decrease the recombination of photogenerated electron and hole pairs (Shifu *et al.,* 2008; Liu *et al.,* 2015). The conjugated polymers can be excited upon visible-light and correct the wide bandgap semiconductors. Also, they are stable photosensitizers

(Wang *et al.,* 2010). Among the conjugated polymers, polyaniline (PANI) has been considered for non-toxicity, corrosion prevention, proper stability, special oxidation-reduction properties, simple synthesis and reasonable prices, high absorption coefficient in the visible region and the high mobility of the load carriers (Saleh and Gupta, 2011; Saleh *et al.,* 2012a; Behniafar *et al.,* 2016; Gu *et al.,* 2016). Meanwhile, supports such as activated carbons, clays, siliceous materials, zeolites and conjugated polymers were applied as adsorption of pollutants (Khani *et al.,* 2010; Padervand *et al.,* 2011; Gupta and Saleh, 2013; Saravanan *et al.,* 2013c; Saravanan *et al.,* 2013d; Gupta *et al.,* 2014a; Sohrabnezhad *et al.,* 2014; Devaraj *et al.,* 2016). PANI can be used as an appropriate adsorbent for removal of pollutants in separation and purification systems also as support for immobilization of photocatalyst. It can increase the adsorption of pollutants (Ai *et al.,* 2010; Di-Paola *et al.,* 2012; Bhaumik *et al.,* 2014; Rajendran *et al.,* 2016; Robati *et al.,* 2016; Saravanan *et al.,* 2015a; Xiong *et al.,* 2013). Herein, Ag_2CO_3 and Ag_2CO_3-PANI were prepared *via* a simple precipitation method. The influences of important parameters such as support amount, pH effect, dye concentration, adsorbent dosage and contact time on the adsorption were investigated. Isotherm, kinetic and thermodynamic models were evaluated *via* the removal of MB as a model dye.

2. Materials and methods

2.1. Materials

Silver nitrate ($AgNO_3$), sodium carbonate (Na_2CO_3), aniline (An) monomer, ammonium persulfate ($(NH_4)_2S_2O_8$, APS), Hydrochloric acid and sodium hydroxide were used. Methylene blue (C.I. name: Basic Blue 9, $C_{16}H_{18}ClN_3S{:}3H_2O$), was used as received.

2.2. Synthesis of Ag_2CO_3, PANI, and Ag_2CO_3-PANI

The synthesis of Ag_2CO_3 was according to the literature (Asadollahi *et al.,* 2017). For polymerization of aniline, 100 mL of freshly distilled aniline monomer with a concentration of 0.2 M was taken in HCl solution and cooled up to 5°C. Then, ammonium persulfate was added into the mixture slowly, and the reaction mixture continues for 4 hours under stirring. The blackish green precipitation after 1 hour was filtered and dried in an oven at 70°C (Saleh and Gupta, 2012b; Ramkumar and Chandramouleeswaran, 2013; Asadollahi *et al.,* 2018). According to the previous work for preparation of Ag_2CO_3-PANI, 0.1 g PANI was dispersed into distilled water. Then, $AgNO_3$ was added to the suspension and was stirred for 1 hour. The Na_2CO_3 solution was added dropwise into the mentioned suspension and stirred for 3 h. The precipitate was collected by centrifugation, thoroughly washed with distilled water and dried at room temperature (Asadollahi *et al.,* 2018).

2.3. Characterization

For determination of functional groups, Fourier transforms infrared (FT-IR) spectra was used on a Brueck spectrophotometer in the 400-4000 cm^{-1} spectral range. The powder X-ray diffraction patterns were recorded by (XRD, Philips PW 1840) from 10° to 70° (2θ). UV–Vis diffuse reflectance spectra (DRS) of the prepared products were taken in the region of 330-950 nm. The morphology and size of the as-synthesized samples were characterized using scanning electron microscopy (SEM) on a JEM-100 CX microscope.

2.4. Evaluation of adsorption efficiency and photo-catalytic activity of sampels

The adsorption and photodegradation of MB dye were investigated for as-prepared PANI and composite. Batch experiments were carried out at a cylindrical pyrex-glass cell with 250 mL capacity. The whole reactor was cooled with a water-cooled jacket on its outside and the temperature was kept at 25°C. At adsorption experiment, the specified amount of composite (0.04-1.2 g/L) was added into 50 mL of aqueous solution of MB (10-100 mg/L) under stirring in the dark for 60 min to complete the adsorption-desorption equilibrium between the dye and the surface of the support and composite. Then, the composites at intervals of 15 min were collected and separated by centrifugation. The filtrate solutions were analyzed spectrophotometrically by measurement of the absorbance at λ = 664 nm.

Owing to the importance of pH, it was the first parameter for investigation at the adsorption experiment. Different amounts of pH were studied. In the adsorption isotherm tests, the initial MB concentrations were investigated. In addition, the effect of contact time and temperature on adsorption was checked out with an assessment of kinetic data and thermodynamic parameters.

After completion of the adsorption-desorption equilibrium between the dye and the surface of the composite, the solution was irradiated with a 200 W tungsten filament Philips lamp (λ ≥ 400 nm) under stirring. In a separate control experiment, the photodegradation of MB was measured under visible light irradiation at λ = 664 nm in the absent of photo-catalyst (photolysis). In the absence of PANI and composite, MB self-degradation was almost negligible under visible light irradiation.

The values of percentage removal (%Removal) and amount of dye adsorbed (q_e) were calculated using the following relationships:

$$\text{Removal}(\%) = \frac{C_0 - C_e}{C_0} \times 100 \quad (1)$$

$$q_e = \frac{(C_0 - C_e)V}{m} \quad (2)$$

Where C_0 and C_e are the initial and equilibrium dye concentration in the liquid phase (mg L^{-1}) respectively, q_e is the amount of MB adsorbed into per unit weight of the adsorbent, V is the volume of the dye solution (L) and m is the mass of the used adsorbent (g) (Ayad and El-Nasr, 2012; Chen *et al.,* 2014).

3. Results

3.1. Characterization of the structure of support, photo-catalyst, and composite

The FT-IR spectra of the PANI and Ag_2CO_3-PANI composite were represented in Figure 1 (Asadollahi *et al.,* 2018). It was observed that after the formation of composite between Ag_2CO_3 and PANI, the absorption bands assigned to all of the vibrations have shifted to higher wavenumbers and the absorption band in 1385 cm^{-1} is assigned to the presence of CO_3^{2-} (Yu *et al.,* 2014). These results confirmed the hybridization of the Ag_2CO_3 and PANI.

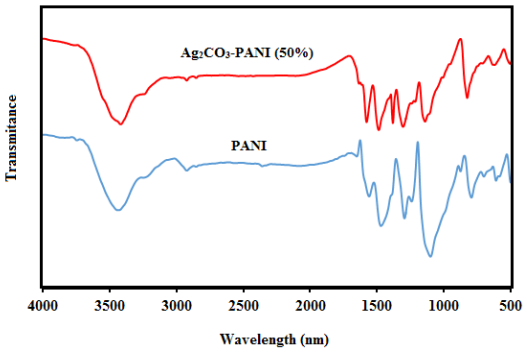

Figure 1. FT-IR spectra of PANI and Ag_2CO_3-PANI (50%) composite

Figure 2 showed the XRD patterns of PANI, Ag_2CO_3 and Ag_2CO_3-PANI composite. In Figure 2a, the broad bands appearing at $2\theta \approx 20^{o}$ and 25^{o} are corresponding to the PANI chains (Jeong *et al.,* 2014; Zhang *et al.,* 2014). The XRD pattern of Ag_2CO_3-PANI was represented in Figure 2b. A short broad peak below $2\theta = 35^{o}$ can be depending on the amorphous nature of the polymer structure (Shifu *et al.,* 2008). Diffraction peaks for monoclinic-phase Ag_2CO_3 were confirmed with XRD patterns (JCPDS No. 26-0339) (Yao and Liu, 2014). For the metallic silver, the peaks at 2θ = 38.32◦, 44.37◦ and 64.67◦ were indicated.

Figure 3 presented DRS spectra of doped PANI, Ag_2CO_3, and Ag_2CO_3-PANI composite. Based on previous studies, the acid-doped form of PANI display three characteristic absorption bands at 320−390, 400−450, and 740−950 nm. The formation of polarons (quinoid segments) of the PANI has happened in the visible range (about 440 nm). Two bands have appeared at 860 nm and 440 nm were related to π–polaron and polaron–π* transition in the acid-doped form of PANI. (Gülce *et al.,* 2013; Che, 2007). For the pure Ag_2CO_3, a wide absorption band from 480-750 nm was assigned to the localized surface plasmon resonance (LSPR) of Ag nanoparticles (Figure 3a) (Dai *et al.,* 2012; Tonda *et al.,* 2015). The absorption band of Ag_2CO_3 and PANI in the Ag_2CO_3-PANI composite were shown in Figure 3b.

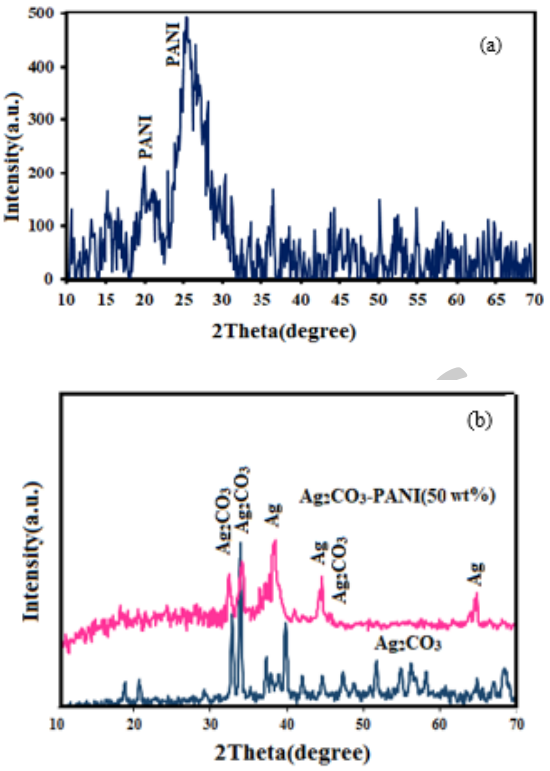

Figure 2. XRD patterns of a) Pani and b) Ag_2CO_3 and Ag_2CO_3-PANI. Inset shows XRD patterns of PANI

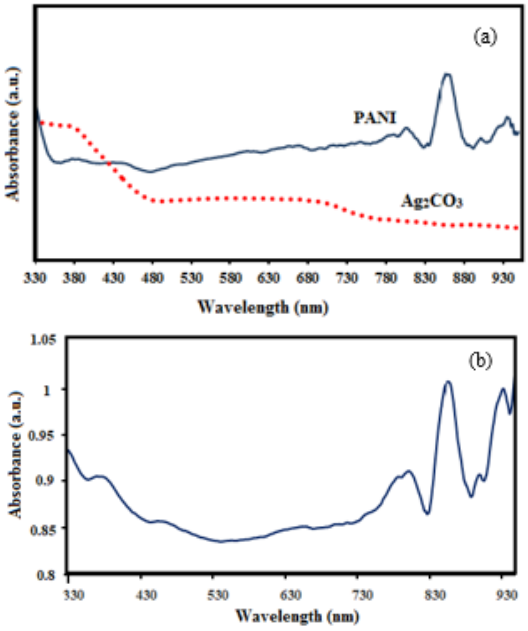

Figure 3. Diffuse reflectance spectra of a) PANI, Ag_2CO_3 and b) Ag_2CO_3-PANI

The morphology and structure of PANI and Ag_2CO_3-PANI samples were characterized by SEM images in Figure 4. According to the SEM images, PANI exhibits a sphere-like morphology (Figure 4a) and Ag_2CO_3 sample with a smooth surface is located along the PANI (Figure 4a).

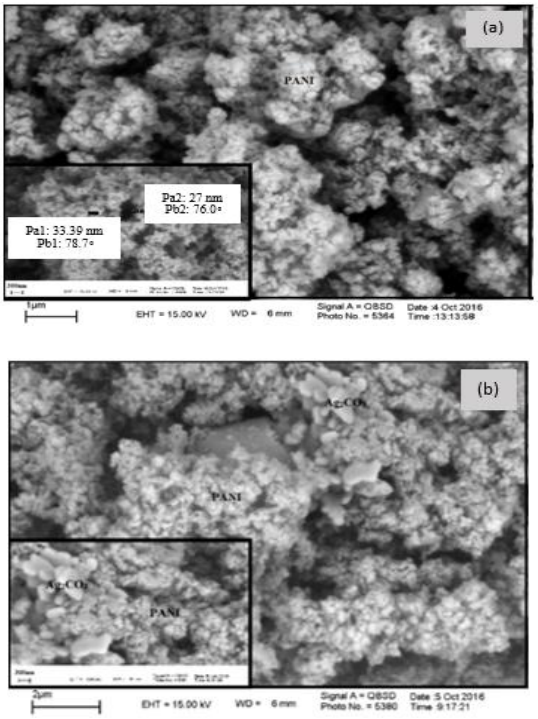

Figure 4. SEM images of the samples (a) PANI; (b) Ag_2CO_3-PANI

3.2. The effect of PANI percentages in composite

The effect of PANI percentages in composite on the removal of MB cationic dye was investigated. Adsorption of PANI was studied in three amounts of pH (pH = 4, 7 and 11). For Ag_2CO_3-PANI composites adsorption and photocatalytic degradation were checked out in two amounts of pH (pH = 7 and 11) with the various percentages of PANI. The adsorption for PANI and the removal efficiency of Ag_2CO_3-PANI (50%) composite were shown in Tables 1 and 2, respectively.

The adsorption of PANI was increased to 98% at alkaline pH but didn't show special adsorption at acidic pH (pH ~3) (Table 1). According to Table 3, for Ag_2CO_3-PANI composites, high removal (adsorption and photodegradation) efficiency were gained under alkaline pH conditions. At alkaline medium, the surface of the composites becomes slightly negatively charged, thus the coordinative interactions with positively charge $R_2 = N^+ = R^/$ group of MB dye is increased. Ag_2CO_3-PANI (50%) composite was selected as an optimal sample because the photocatalytic degradation of dye increased in this sample (Saravanan *et al.,* 2015b). In other samples with higher percentages of PANI decrease in photocatalytic activity may be the result of the reduction of the amount of photocatalyst in composite due to a large amount of support in the sample.

Table 1. The adsorption for PANI sample (C_{MB} = 50 mg L^{-1}, the amounts of PANI: 1 g L^{-1}, adsorption time: 60 min, T: 32 °C)

	%Adsorption
	8 (The solution natural pH = 3)
PANI	60 (pH = 7)
	98.5 (pH = 11)

3.3. The effect of pH

The pH_{PZC} can be determined using the immersion technique. The adsorption of anions and cations is favored at pH < pH_{PZC} and pH > pH_{PZC}, respectively (Chingombe *et al.,* 2005; Zheng *et al.,* 2012). Using the immersion technique the pH_{PZC} values for PANI and composite were determined 10.5 and 6.5. The pH studies for PANI and Ag_2CO_3-PANI are summarized in Table 3. At the alkaline pH, samples were increasingly deprotonated, thus adsorption of dye was increased. The positively charged dye is attracted to the negatively charged surface sites of the PANI and Ag_2CO_3-PANI (50%) at pH = 10.

Table 2. The effect of different weight percentages of PANI in composite on adsorption, photodegradation efficiency and removal for Ag_2CO_3-PANI samples (C_{MB} = 50 mg L^{-1}, the amounts of Ag_2CO_3-PANI (50%): 1 g L^{-1}, adsorption time: 60 min, photocatalytic degradation time: 90 min, T: 32 °C)

	Ag_2CO_3-PANI (10%)	**Ag_2CO_3-PANI (30%)**	**Ag_2CO_3-PANI (50%)**	**Ag_2CO_3-PANI (60%)**	**Ag_2CO_3-PANI (80%)**
%Adsorption (The solution natural pH)	0	3	10	8	3
%Adsorption (pH = 11)	8.5	45	81.4	94	98.1
%Photodegradation (pH = 11)	24	27.5	87.4	54.7	0
% Removal (pH = 11)	32	60.9	97.7	98	98.1

Table 3. The effect of pH on adsorption, photodegradation efficiency and removal for Ag_2CO_3-PANI sample (50%) in (C_{MB} = 50 mg L^{-1}, the amounts of Ag_2CO_3 and Ag_2CO_3-PANI (50%): 1 g L^{-1}, adsorption time: 60 min, photocatalytic degradation time: 90 min, T: 32 °C)

	pH = 3	**pH = 6**	**pH = 7**	**pH = 9**	**pH = 10**	**pH = 11**
%Adsorption for PANI	8.24	32	60	87.32	98	98.5
q_e of PANI (mg g^{-1})	4.12	15.2	27.91	40.48	45.6	45.65
%Adsorption for Ag_2CO_3-PANI (50%)	0	9.76	43.67	57	62.85	81.40
q_e of Ag_2CO_3-PANI(50%)	0	4.7	22	28.88	30.17	39.18
%Phothodegradation for Ag_2CO_3-PANI (50%)	0	0	48.83	55	85.75	87.38
% Removal for Ag_2CO_3-PANI (50%)	0	9.76	71.29	80	94.38	97.67

According to Table 3, adding of Ag_2CO_3 into PANI cause to decrease the percentage and capacity adsorption for composite rather than the pure support but the comparison of %adsorption for PANI and removal percentage for Ag_2CO_3-PANI (50%) indicated that there isn't any significant difference between adsorbents at pH≥10. Thus pH = 10 was selected as optimized pH.

3.4. Effect of different composite dosages on the removal of MB dye by Ag_2CO_3-PANI (50%) composite

For investigating the effect of composite dosage on the adsorption of MB dye, different weights of Ag_2CO_3-PANI (50%) varied between 0.02 and 0.06 g were exposed to the 50 mL of the dye solution with 50.0 mg/L concentration for 60 min in the dark and 90 min under a light. The other operational parameters were kept at the optimum (pH = 10). The obtained results have been summarized in Table 4 and Figure 5, respectively.

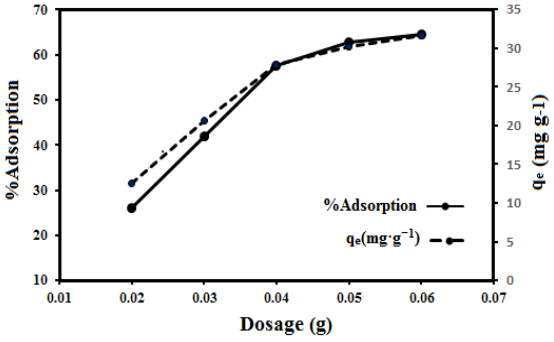

Figure 5. Effect of adsorbent dosage on q_e and adsorption percentage of MB by Ag_2CO_3-PANI (50%)

Table 4. The effect of adsorbent dosage on % adsorption, % photodegradation and % removal of MB by Ag_2CO_3-PANI (50%) Adsorption experiments (C_0 = 50 mg L^{-1}, PANI and Ag_2CO_3-PANI (50%), equilibration time = 60 min, T = 32 °C, pH = 10)

Dosage(g)	%Adsorption	q_e	%Photodegradation	%Removal
0.02	26.14	12.52	36.4	53
0.03	42	20.62	50	71
0.04	57.6	27.94	65.3	85.29
0.05	62.85	30.17	85.75	94.38
0.06	64.6	31.65	76.2	95.81

As seen in Figure 10 %adsorption is increased gradually with increasing the amount of sorbent due to increase in sportive surface area and availability of more exchangeable sites for dy (Asfaram *et al.,* 2015; Gupta *et al.,* 2014b). Adsorption of dye was observed at 62.85% for 0.050 g of the composite dosage and then increased slowly but photodegradation percent was decreased when 0.060 g of the composite was employed. This reduction could be attributed to the turbidity of solution and diminution of incident radiation into photo-catalyst (Saravanan *et al.,* 2013e).

4. Discussion

4.1. Adsorption kinetics

The adsorption kinetics was used for determination of the optimum time for the adsorption of MB by PANI and Ag_2CO_3-PANI (50%). Figure 5 shows the effect of contact time on the adsorption of MB onto PANI and Ag_2CO_3-PANI (50%) composite. As it is shown, the adsorption capacity for PANI increases rapidly and reaches equilibrium after 30 min, while for Ag_2CO_3-PANI (50%), this time is prolonged to 60 min.

In order to evaluate the adsorption behavior of MB by the used adsorbents, the pseudo-first-order and pseudo-second-order models were applied to interpret the experimental data, as shown below (Lagergren, 1898; Ho and McKay, 1998):

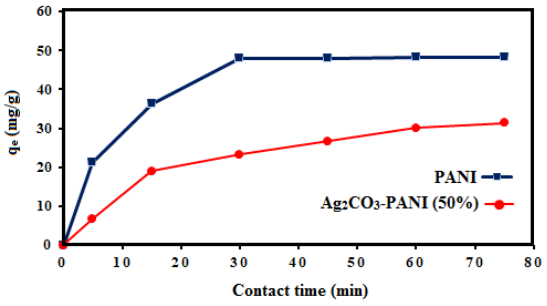

Figure 6. Effect of contact time on adsorption capacity of MB using PANI and Ag_2CO_3-PANI (50%). Adsorption experiments (C_0 = 50 mg L^{-1}, pH = 10, PANI and Ag_2CO_3-PANI (50%) dosage = 1 g L^{-1}, equilibration time = 60 min, T = 32 °C)

Pseudo-first-order equation:

$$\mathrm{Log}(q_e - q_t) = \log q_e - k_1/2.303 \quad (3)$$

Pseudo-second-order equation:

$$\frac{t}{q_t} = \frac{1}{k_2 q_e^2} + \frac{t}{q_e} \quad (4)$$

Where q_e and q_t are the amounts of dye adsorbed (mg g^{-1}) at equilibrium, t is the exposure time (min) and K is the rate constant, respectively. The validities of kinetic models are checked and verified by the linear equation analysis in Figure 7(a, b).

The kinetic parameters (k_1, k_2 and q_e), and the correlation coefficients (R_2) values were determined and summarized in Table 5.

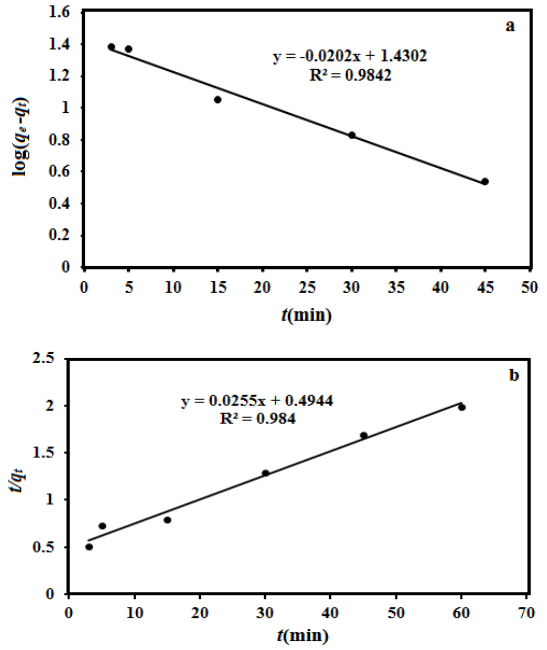

Figure 7. Adsorption kinetic MB onto PANI and Ag_2CO_3-PANI (50%): (a) pseudo-first order model, (b) pseudo-second order model (C_0 = 50 mg L^{-1}, PANI and Ag_2CO_3-PANI (50%) dosage = 1 g L^{-1}, equilibration time = 60 min, T = 32 °C)

Table 5. Kinetic parameters for the adsorption of MB onto Ag_2CO_3-PANI (50%) composite (C_0 = 50 mg L^{-1}, pH = 10, PANI and Ag_2CO_3-PANI (50%) dosage = 1 g L^{-1}, equilibration time = 60 min, T = 32 °C)

Models	Model coefficients	R^2
Pseudo-first-order	$q_{e,cal}$ =27 mg g^{-1} $q_{e,exp}$ = 30.17 mg g^{-1} k_1 = 0.0465 min^{-1}	0.9842
Pseudo-second-order	q_e = 39.22 mg g^{-1} k_2 = 0.0013 g mg^{-1} min^{-1}	0.984

Good correlation with the kinetic data explains the dye adsorption mechanism in the solid phase. There is no significant difference between R^2 for the pseudo-first-order model and the pseudo-second-order model, while the obtained $q_{e,cal}$ value was very close to the $q_{e,exp}$ value for the pseudo-first-order model, implying that the pseudo-first-order model is suitable for describing the adsorption kinetics of MB onto Ag_2CO_3-PANI(50%) photo-catalyst (Ai *et al.,* 2010; Karthikeyan *et al.,* 2012; Xiong *et al.,* 2013). As shown in Figure 7 for PANI and Ag_2CO_3-PANI (50%) the external surface adsorption is very fast before 15 min. Then, the adsorption increased very slowly. This observation can be justified in this way: the saturation of the active sites decreases the rate of adsorption after 15 min.

4.2. Adsorption isotherm

The results of initial concentration studies of dye on the percentages of adsorption, photodegradation, and removal of MB by PANI and Ag_2CO_3-PANI (50%) are summarized in Table 6.

Table 6. The effect of initial concentration on %adsorption, %photodegradation and % removal of MB by Ag_2CO_3-PANI (50%). (the amount of Ag_2CO_3-PANI (50%): 1 g L^{-1}, adsorption time = 60 min, photocatalytic degradation time = 90 min, T: 32 ºC)

Support and catalyst	C_0 = 30 mg L^{-1}	C_0 = 50 mg L^{-1}	C_0 = 60 mg L^{-1}	C_0 = 80 mg L^{-1}	C_0 = 100 mg L^{-1}
%Adsorption for Ag_2CO_3-PANI (50%)	75.96	62.85	63	55.08	43.29
%Photodegradation for Ag_2CO_3-PANI (50%)	68.24	85.75	65.42	61.92	56.79
% Removal for Ag_2CO_3-PANI (50%)	92.3	94.38	87.2	82.89	75.5

The adsorption isotherm models were applied to determine the specific relation between the concentration of adsorbate and the adsorption capacity of adsorbent, the maximum adsorption capacity of adsorbent and predictive modeling for analysis and design of adsorption systems. Two important isotherms (The Langmuir and Freundlich isotherm models) were selected to describe the mechanism of the adsorption process. The linear equation of the Langmuir (Eq. 5), Freundlich (Eq. 6) isotherm models are expressed as follows (Ai *et al.,* 2010; Ansari *et al.,* 2011; Bhaumik *et al.,* 2014; Xiong *et al.,* 2013):

$$\frac{1}{q_e} = \frac{1}{q_m} + \frac{1}{bq_mC_e} \quad (5)$$

$$\mathrm{Log}\, q_e = \log k_f + \frac{1}{n}\log C_e \quad (6)$$

Where the constant b is related to the energy of adsorption (L mg^{-1}), and q_m is the Langmuir monomolecular adsorption capacity (mg g^{-1}); k_f ($mg^{(1-1/n)}$ g^{-1} L^{-n}) and n are the Freundlich constants related to adsorption capacity (mg g^{-1}) and intensity of adsorption, respectively. The n value between 2 and 10 indicates that the adsorption system is desirable, between 1 and 2 is fairly difficult, and less than 1 is poor (Yao *et al.,* 2010).

Figure 8(a, b) shows a linear plot of $1/q_e$ against $1/C_e$ for Langmuir isotherm and log q_e against log C_e for Freundlich isotherm. The Langmuir and Freundlich isotherm parameters were summarized in Table 7.

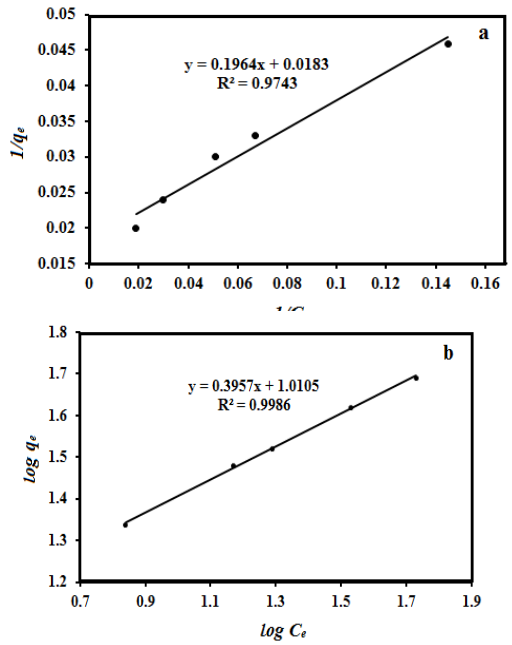

Figure 8. Adsorption isotherm models: (a) linear Langmuir model (b) linear Fruendlich model for MB adsorption

The Langmuir isotherm makes several assumptions, such as the monolayer adsorption occurs on specific homogeneous sites of the adsorbent. The essential characteristics of the Langmuir isotherm can be expressed in terms of a dimensionless constant that called the separation factor or equilibrium parameter R_L and defined by the (Eq. 7).

$$R_L = \frac{1}{(1+bC_0)} \quad (7)$$

The R_L value indicates the shape of the isotherm: $R_L > 1$ (unfavorable isotherm), $R_L = 1$ (linear isotherm), $0 < R_L < 1$ (favorable isotherm), $R_L = 0$ (irreversible isotherm) (Foo and Hameed, 2010). Another isotherm for adsorption processes on heterogeneous surfaces is the Freundlich isotherm that can be used for non-ideal adsorption. The calculated R_L values are in the range of 0.102-0.272 indicating that MB adsorption onto the Ag_2CO_3-PANI (50%) is favorable (Figure 9).

Table 7. Isotherm parameters for the Adsorption of MB onto Ag_2CO_3-PANI (50%) composite

	Langmuir			Freundlich		
Catalyst	**q_m (mg g^{-1})**	**b (L mg^{-1})**	**R^2**	**K_f (mg g^{-1})**	**n**	**R^2**
Ag_2CO_3-PANI (50%)	55	0.091	0.976	9.97	2.53	0.999

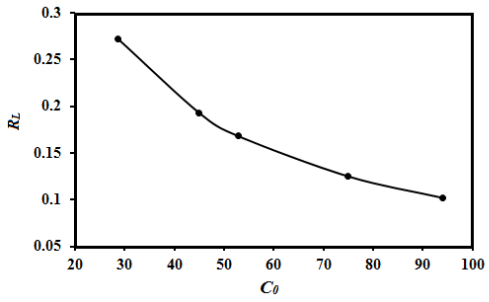

Figure 9. The plot of R_L value *vs.* C_0 for linear Langmuir model

The higher value of correlation coefficients (R^2) obtained for the Freundlich model (0.999) indicates that the Freundlich model fitted with the isotherm data better than the Langmuir model (R^2 = 0.976). Furthermore, the calculated n value (2.53) indicates that the Freundlich model is favorable for describing the adsorption process. These results are in good agreement with the Pseudo-first-order model in kinetics studies.

Here, it should be mentioned that the adsorption capacity of Ag_2CO_3 for MB is negligible compared to PANI. Then it is anticipated that compared with PANI, the Ag_2CO_3-PANI (50%) will exhibit a decreasing adsorption capacity for MB. However, the decreased percentage is far less than the Ag_2CO_3 content in Ag_2CO_3-PANI (50%). As seen in Figure 10, if the adsorption capacity is calculated based on per gram of PANI, the adsorption capacity of Ag_2CO_3-PANI (50%) for MB is observed to be higher than that of PANI (Zheng *et al.,* 2012).

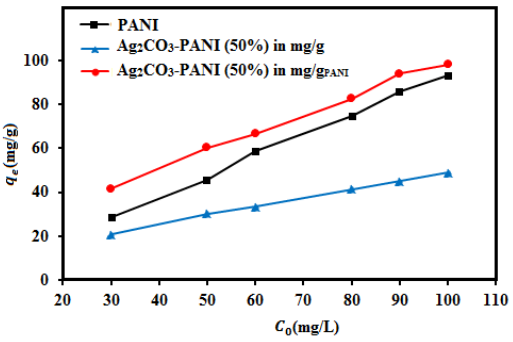

Figure 10. The plot of the adsorption capacity against initial concentration of MB. Adsorption experiments (C_0 = 50 mg L^{-1}, PANI and Ag_2CO_3-PANI (50%) dosage = 1 g L^{-1}, equilibration time = 60 min, T = 32 °C, pH = 10)

The comparison of the adsorbent capacity of different low cost and commercially available adsorbents is shown in Table 8. When compared with other adsorbents, the results of the present study indicate that Ag_2CO_3-PANI composite as an adsorbent has better adsorption capacity in almost all cases and proves to be a cost-effective adsorbent that can be used for the removal of Methylene Blue cationic dyes from aqueous solution.

Table 8. The maximum adsorption capacity of various commercial adsorbents

Adsorbents	Adsorption Capacity (mg/g)	Reference
Polyacrylonitrile (PAN) based activated carbon nanofibers (ACNFs)	72.46	(Ibupoto *et al.,* 2018)
Graphene nanosheet/magnetite (Fe_3O_4) composite	43.82	(Ai *et al.,* 2011a)
Carbonized citrus fruit peel	25.51	(Dutta *et al.,* 2011)
Fly ash	5.72	(Kumar *et al.,* 2005)
Magnetite-loaded multi-walled carbon nanotubes (M-MWCNTs)	48.06	(Ai *et al.,* 2011b)
Fe_3O_4@ZIF8-heterostructure	20.20	(Zheng *et al.,* 2014)
Raw KT3B kaolin (Algeria)	52.76	(Mouni *et al.,* 2018)
Natural zeolite	21.78	(Wang *et al.,* 2006)
Zeolites from kaolin (Egypt)	11.13 to 21.41	(EL-Mekkawi *et al.,* 2016)
Ag_2CO_3-PANI composite	55.00	Present study

4.3. Thermodynamic parameters

The thermodynamic studies were performed with calculation of the change in Gibb's free energy (ΔG°), the change in entropy (ΔS°) and the change in enthalpy (ΔH°) for adsorbent using following relations (Mohammadi *et al.,* 2011; Zheng *et al.,* 2012):

$$\Delta G^0 = -RTLnK_C \quad (8)$$

$$\Delta G^0 = \Delta H^0 - T\Delta S^0 \quad (9)$$

$$K_C = \frac{C_{Ae}}{C_e} \quad (10)$$

$$LnK_C = -\frac{\Delta H^0}{RT} + \frac{\Delta S^0}{R} \quad (11)$$

Where T is the absolute temperature in Kelvin (K), K_C is the equilibrium constant, C_{Ae} is the amount of dye adsorbed on the adsorbent per liter of the solution at equilibrium (mg L^{-1}), C_e is the equilibrium concentration of the dye in the solution (mg L^{-1}) and R is the gas constant (8.314 J mol^{-1} K^{-1}). The plot of LnK_c against 1/T (1 K^{-1}) (the van't Hoff plot) was be used to calculate thermodynamic adsorption parameters (ΔH° and ΔS°) at solid-solution interface (Vadivelan and Kumar, 2005). The van't Hoff plot for the adsorption of MB onto Ag_2CO_3-PANI (50%) is given in Figure 11. The calculated values of the thermodynamic parameters are calculated and presented in Table 9.

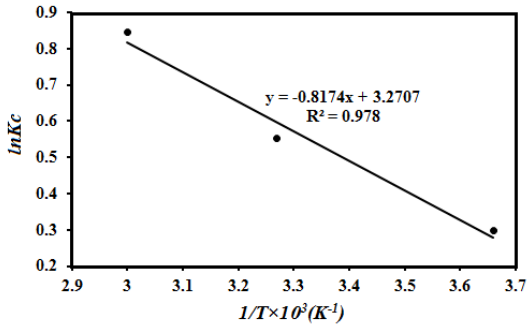

Figure 11. The plot of lnK_c against reciprocal temperature for the adsorption of MB by Ag_2CO_3-PANI (50%). Adsorption experiments: C_0 = 50 mg L^{-1}, t = 60 min; pH = 10, adsorbent amount = 1 g L^{-1}

Table 9. The adsorption and photodegradation efficiency for Ag_2CO_3-PANI (50%) samples in different temperature. Adsorption experiments = 1 g L^{-1}, C_{MB} = 50 mg L^{-1}, pH = 10, adsorption time = 60 min, photocatalytic degradation time = 90 min)

T (K)	%Adsorption	%Photodegradation	%Removal
273	57.4	48.49	79.43
306	63.43	72.65	90
333	70	83.36	94.65

Table 10 indicates thermodynamic parameters for the adsorption of MB by Ag_2CO_3-PANI (50%). The negative values of ΔG° for the MB adsorption on Ag_2CO_3-PANI (50%) at different temperatures indicate the spontaneous nature and feasibility of the process adsorption. The increase in -ΔG° indicated that the adsorption of MB on composite was more at the higher temperature. However, the moderate slope of lnK_c T^{-1} curve indicated that the temperature doesn't have a major effect on the adsorption process. The negative values of ΔG° for physisorption processes are usually between −20 and 0 kJ/mol, whereas that for chemisorption processes is often in the range of −80 to −400 kJ mol^{-1}. This result was approved by the small numerical value of ΔH°. The positive value for enthalpy changes reveals the endothermic nature of adsorption and it shows the possibility of physical adsorption (the electrostatic attractions such as dipole-dipole, dispersion, London-Vander Waals and H-bonding). The positive value of ΔS° shows the increased randomness at the solid/solution interface (due to replacement of some hydration water molecules adsorbed on the surface of adsorbent with the dye molecules) and reflects the affinity of the Ag_2CO_3-PANI (50%) for MB dye (Ansari *et al.,* 2011; Kara *et al.,* 2015).

4.4. Regeneration and reusability of Ag_2CO_3-PANI (50%)

According to the previous results, the adsorption of MB on Ag_2CO_3-PANI (50%) was a physical process. Thus desorption is expected to occur under the neutral or the acidic environments. In addition, some of the

adsorbed MB dye molecules photodegraded in the presence of photo-catalyst, so the calculated desorption percentage was lower than the expected value. One procedure for batch desorption of dye was as follows: at first, the adsorption experiment was done in ideal condition, and then the used composite in adsorption process was collected by centrifuge and dried at room temperatures. The dried solid was then added into the deionized water and then the acidic solution in two steps with stirring in dark for 1 hour. It was observed that a large amount of the previously adsorbed dye the composite was desorbed. Desorption efficiency was measured using the following equations (Zhao *et al.,* 2011; Christopher *et al.,* 2012; Ansari *et al.,* 2013; Yan *et al.,* 2016):

$$\text{Desorption ratio} = \frac{\text{Amount of dye desorbed to the desorption medium(m*)}}{\text{Amount of dye adsorbed on the composite}(m_o)} \times 100 \quad (12)$$

$$m^* = C_e \times V' \quad (13)$$

$$m_0 = (C_0 - C_e) \times V \quad (14)$$

Where, m_0 (mg) of the adsorbed dye onto the adsorbent, m* (mg) of the released dye in the regenerated solution; V′ is the volume of eluent solution (L). C_0 and C_e are the initial (inlet) and equilibrium (outlet) concentrations (mg L^{-1}) of dye, respectively (Mehraj *et al.,* 2014; Shang *et al.,* 2009). The results indicated the regeneration of up to 97% from an adsorbed dye, using water and 0.1 M HCl.

Table 10. Thermodynamic parameters for the adsorption of MB by Ag_2CO_3-PANI (50%)

T (K)	K_c	-ΔG° (J mol^{-1})	ΔH° (KJ mol^{-1})	ΔS° (J mol^{-1} K^{-1})
273	1.347	0.756	0.0067	0.0272
306	1.734	1.653		
333	2.330	2.388		

5. Conclusion

A highly efficient Ag_2CO_3-PANI heterojunction has been prepared successfully by a facile precipitation method. The using PANI with Ag_2CO_3 influenced the adsorption capacity and the degradation rate of dye molecules on the surface of the composite. The Freundlich isotherm model provided the best fits to predict the adsorption equilibrium for the MB onto the photocatalyst. The kinetic study confirmed the pseudo-first-order model for the adsorption process. Owning to the thermodynamic study the adsorption process was spontaneous and endothermic (ΔG < 0 and ΔH > 0). The adsorption-desorption cycle experiments demonstrated the possibility of desorption for frequent application. The excellent photocatalytic activity for the degradation of MB was superior to those of pure Ag_2CO_3 and PANI under visible light irradiation. Thus PANI as a good support influences on photocatalytic activity and stability of photocatalyst and provide a promising insight into the application of various photosensitive Ag-based materials with enhanced adsorption, photocatalytic activity, and photo stability.

Acknowledgments

The authors are thankful to the post-graduate office of Guilan University for the financial support of this work.

References

Ayad M.M. and El-Nasr A.A. (2012), Anionic dye (acid green 25) adsorption from water by using polyaniline nanotubes salt/silica composite, *Journal of Nanostructure in Chemistry*, **3**, 3.

Ai L., Jiang J. and Zhang R. (2010), Uniform polyaniline microspheres: a novel adsorbent for dye removal from aqueous solution, *Synthetic Metals*, **160**, 762-767.

Ai L., Zhang C. and Jiang J. (2013), Hierarchical porous AgCl@ Ag hollow architectures: self-templating synthesis and highly enhanced visible light photocatalytic activity, *Applied Catalysis B: Environmental*, **142**, 744-751.

Ai L., Zhang C. and Chen Z. (2011a), Removal of methylene blue from aqueous solution by a solvothermal-synthesized graphene/magnetite composite, *Journal of Hazardous Materials*, **192**(3), 1515-1524.

Ai L., Zhang C., Liao F., Wang Y., Li M., Meng L. and Jiang J. (2011b), Removal of methylene blue from aqueous solution with magnetite loaded multi-wall carbon nanotube: kinetic, isotherm and mechanism analysis, *Journal of Hazardous Materials*, **198**, 282-290.

Ansari R., Keivani M.B. and Delavar A.F. (2011), Application of polyaniline nanolayer composite for removal of tartrazine dye from aqueous solutions, *Journal of Polymer Research*, **18**, 1931-1939.

Asfaram A., Ghaedi M., Agarwal S., Tyagi I. and Gupta V.K. (2015), Removal of basic dye Auramine-O by ZnS: Cu nanoparticles loaded on activated carbon: optimization of parameters using response surface methodology with central composite design, *RSC Advances*, **5**(24), 18438-18450.

Asadollahi A., Sohrabnezhad S., Ansari R. and Zanjanchi M.A. (2018), pn heterojuction in organic (polyaniline)-inorganic (Ag_2CO_3) polymer-based heterojuction photocatalyst, *Materials Science in Semiconductor Processing*, **87**, 119-125.

Asadollahi A., Sohrabnezhad S. and Ansari R. (2017), Enhancement of photocatalytic activity and stability of Ag_2CO_3 by formation of AgBr/Ag_2CO_3 heterojunction in mordenite zeolite, *Advanced Powder Technology*, **28**, 304-313.

Ansari R., Mohammad-khah A. and Nazmi M. (2013), Application of chemically modified beach sand as low cost efficient adsorbent for dye removal, *Current Chemistry Letters*, **2**, 215-223.

Ahmaruzzaman M. and Gupta V.K. (2011), Rice husk and its ash as low-cost adsorbents in water and wastewater treatment, *Industrial & Engineering Chemistry Research*, **50**(24), 13589-13613.

Bao N., Li Y., Wei Z., Yin G. and Niu J. (2011), Adsorption of dyes on hierarchical mesoporous TiO_2 fibers and its enhanced photocatalytic properties, *The Journal of Physical Chemistry C*, **115**, 5708-5719.

Behniafar H., Malekshahinezhad K. and Alinia-pouri A. (2016), One-pot methods for preparing polyaniline/Ag nanocomposites via oxidative polymerization of aniline, *Journal of Materials Science: Materials in Electronics*, **27**, 1070-1076.

Bhaumik M., Choi H.J., McCrindle R.I. and Maity A. (2014), Composite nanofibers prepared from metallic iron nanoparticles and polyaniline: high performance for water treatment applications, *Journal of Colloid and Interface Science*, **425**, 75-82.

Cheng J., Chang P.R., Zheng P. and Ma X. (2014), Characterization of magnetic carbon nanotube–cyclodextrin composite and its adsorption of dye, *Industrial & Engineering Chemistry Research*, **53**, 1415-1421.

Crini G. (2006), Non-conventional low-cost adsorbents for dye removal: a review, *Bioresource Technology*, **97**, 1061-1085.

Che C.M. (2007), Nanocomposite field effect transistors based on zinc oxide/polymer blends, *In Microprocesses and Nanotechnology*, 104-105

Chingombe P., Saha B. and Wakeman R.J. (2005), Surface modification and characterisation of a coal-based activated carbon, *Carbon*, **43**, 3132-3143.

Christopher P., Xin H., Marimuthu A. and Linic S. (2012), Singular characteristics and unique chemical bond activation mechanisms of photocatalytic reactions on plasmonic nanostructures, *Nature Materials*, **11**, 1044.14.

Dai G., Liu S., Liang Y. and Liu K. (2014), Fabrication of a nano-sized Ag_2CO_3/reduced graphene oxide photocatalyst with enhanced visible-light photocatalytic activity and stability, *RSC Advances*, **4**, 34226-34231.

Dai G., Yu J. and Liu G. (2012), A new approach for photocorrosion inhibition of Ag_2CO_3 photocatalyst with highly visible-light-responsive reactivity, *The Journal of Physical Chemistry C*, **116**, 15519-15524.

Devaraj M., Saravanan R., Deivasigamani R., Gupta V.K., Gracia F. and Jayadevan S. (2016), Fabrication of novel shape Cu and Cu/Cu_2O nanoparticles modified electrode for the determination of dopamine and paracetamol, *Journal of Molecular Liquids*, **221**, 930-941.

Di-Paola A., García-López E., Marcì G. and Palmisano L. (2012), A survey of photocatalytic materials for environmental remediation, *Journal of Hazardous Materials*, **211**, 3-29.

Dutta S., Bhattacharyya A., Ganguly A., Gupta S. and Basu S. (2011), Application of response surface methodology for preparation of low-cost adsorbent from citrus fruit peel and for removal of methylene blue, *Desalination*, **275**(1), 26-36.

EL-Mekkawi D.M., Ibrahim F.A. and Selim M.M. (2016), Removal of methylene blue from water using zeolites prepared from Egyptian kaolins collected from different sources, *Journal of Environmental Chemical Engineering*, **4**(2), 1417-1422.

Foo K.Y. and Hameed B.H. (2010), Insights into the modeling of adsorption isotherm systems, *Chemical Engineering Journal*, **156**, 2-10.

Ghaedi M., Hajjati S., Mahmudi Z., Tyagi I., Agarwal S., Maity A. and Gupta V.K. (2015), Modeling of competitive ultrasonic assisted removal of the dyes–Methylene blue and Safranin-O using Fe_3O_4 nanoparticles, *Chemical Engineering Journal*, **268**, 28-37.

Gu Z.J. and Shen Q. (2016), Synthesis, characterization and comparison of polyaniline 1D-structure controlled by poly (L-lactide) and poly (D-lactide), *Superlattices and Microstructures*, **89**, 53-58.

Gülce H., Eskizeybek V., Haspulat B., Sarı F., Gülce A. and Avcı A. (2013), Preparation of a new polyaniline/CdO nanocomposite and investigation of its photocatalytic activity: comparative study under UV light and natural sunlight irradiation, *Industrial & Engineering Chemistry Research*, **52**, 10924-10934.

Gupta V.K., Jain R., Nayak A., Agarwal S. and Shrivastava M. (2011), Removal of the hazardous dye—tartrazine by photodegradation on titanium dioxide surface, *Materials Science and Engineering: C*, **31**(5), 1062-1067.

Gupta V.K., Kumar R., Nayak A., Saleh T.A. and Barakat M.A. (2013), Adsorptive removal of dyes from aqueous solution onto carbon nanotubes: a review, *Advances in Colloid and Interface Science*, **193**, 24-34.

Gupta V.K., and Saleh T.A. (2013), Sorption of pollutants by porous carbon, carbon nanotubes and fullerene-An overview, *Environmental Science and Pollution Research*, **20**(5), 2828-2843.

Gupta V.K., Nayak A., Agarwal S. and Tyagi I. (2014; a), Potential of activated carbon from waste rubber tire for the adsorption of phenolics: Effect of pre-treatment conditions, *Journal of Colloid and Interface Science*, **417**, 420-430.

Gupta V.K., Atar N., Yola M.L., Üstündağ Z. and Uzun L. (2014b), A novel magnetic Fe@ Au core–shell nanoparticles anchored graphene oxide recyclable nanocatalyst for the reduction of nitrophenol compounds, *Water Research*, **48**, 210-217.

Gupta V.K., Nayak A. and Agarwal S. (2015), Bioadsorbents for remediation of heavy metals: current status and their future prospects, *Environmental Engineering Research*, **20**(1), 1-18.

Ho Y.S. and McKay G. (1998), Sorption of dye from aqueous solution by peat, *Chemical Engineering Journal*, **70**, 115-124.

Jeong W.H., Amna T., Ha Y.M., Hassan M.S., Kim H.C. and Khil M.S. (2014), Novel PANI nanotube@ TiO_2 composite as efficient chemical and biological disinfectant, *Chemical Engineering Journal*, **246**, 204-210.

Khani H., Rofouei M.K., Arab P., Gupta V.K. and Vafaei Z. (2010), Multi-walled carbon nanotubes-ionic liquid-carbon paste electrode as a super selectivity sensor: application to potentiometric monitoring of mercury ion (II), *Journal of Hazardous Materials*, **183**(1-3), 402-409.

Karthikeyan S., Gupta V.K., Boopathy R., Titus A. and Sekaran G. (2012), A new approach for the degradation of high concentration of aromatic amine by heterocatalytic Fenton oxidation: kinetic and spectroscopic studies, *Journal of Molecular Liquids*, **173**, 153-163.

Kumar K.V., Ramamurthi V. and Sivanesan S. (2005), Modeling the mechanism involved during the sorption of methylene blue onto fly ash, *Journal of Colloid and Interface Science*, **284**(1), 14-21.

Kara A., Demirbel E., Tekin N., Osman B. and Beşirli N. (2015), Magnetic vinylphenyl boronic acid microparticles for Cr (VI) adsorption: Kinetic, isotherm and thermodynamic studies, *Journal of Hazardous Materials*, **286**, 612-623.

Liu B., Fang Y., Li Z. and Xu S. (2015), Visible-light nanostructured photocatalysts—a review, *Journal of Nanoscience and Nanotechnology*, **15**, 889-920.

Lagergren S.K. (1898), About the theory of so-called adsorption of soluble substances, *Svenska Vetenskapsakademiens Handlingar*, **24**, 1-39.

Ibupoto A.S., Qureshi U.A., Ahmed F., Khatri Z., Khatri M., Maqsood M., Brohi R.Z. and Kim I.S. (2018), Reusable carbon nanofibers for efficient removal of methylene blue from aqueous solution, *Chemical Engineering Research and Design*, **136**, 744-752.

Mittal A., Mittal J., Malviya A. and Gupta V.K. (2010), Removal and recovery of Chrysoidine Y from aqueous solutions by waste materials, *Journal of Colloid and Interface Science*, **344**(2), 497-507.

McEvoy J.G. and Zhang Z. (2014), Antimicrobial and photocatalytic disinfection mechanisms in silver-modified photocatalysts under dark and light conditions, *Journal of Photochemistry and Photobiology C: Photochemistry Reviews*, **19**, 62-75.

Mohammadi N., Khani H., Gupta V.K., Amereh E. and Agarwal S. (2011), Adsorption process of methyl orange dye onto mesoporous carbon material–kinetic and thermodynamic studies, *Journal of Colloid and Interface Science*, **362**(2), 457-462.

Mehraj O., Mir N.A., Pirzada B.M., Sabir S. and Muneer M. (2014), In-situ anion exchange synthesis of $AgBr/Ag_2CO_3$ hybrids with enhanced visible light photocatalytic activity and improved stability, *Journal of Molecular Catalysis A: Chemical,* **395**, 16-24.

Mouni L., Belkhiri L., Bollinger J.C., Bouzaza A., Assadi A., Tirri A., Dahmoune F., Madani Kh. and Remini H. (2018), Removal of methylene blue from aqueous solutions by adsorption on kaolin: kinetic and equilibrium studies, *Applied Clay Science*, **153**, 38-45.

Padervand M., Tasviri M. and Gholami M.R. (2011), Effective photocatalytic degradation of an azo dye over nanosized Ag/AgBr-modified TiO_2 loaded on zeolite, *Chemical Papers*, **65**, 280-288.

Ramkumar J. and Chandramouleeswaran S. (2013), Separation of uranyl ion using polyaniline, *Journal of Radioanalytical and Nuclear Chemistry*, **298**, 1543-1549.

Rajendran S., Khan M.M., Gracia F., Qin J., Gupta V.K. and Arumainathan S. (2016), Ce^{3+}-ion-induced visible-light photocatalytic degradation and electrochemical activity of ZnO/CeO_2 nanocomposite, *Scientific Reports*, **6**, 31641.

Robati D., Mirza B., Rajabi M., Moradi O., Tyagi I., Agarwal S. and Gupta V.K. (2016), Removal of hazardous dyes-BR 12 and methyl orange using graphene oxide as an adsorbent from aqueous phase, *Chemical Engineering Journal*, **284**, 687-697.

Saleh T.A. and Gupta V.K. (2012a), Photo-catalyzed degradation of hazardous dye methyl orange by use of a composite catalyst consisting of multi-walled carbon nanotubes and titanium dioxide, *Journal of Colloid and Interface Science*, **371**(1), 101-106.

Saleh T.A. and Gupta V.K. (2012b), Synthesis and characterization of alumina nano-particles polyamide membrane with enhanced flux rejection performance, *Separation and Purification Technology*, **89**, 245-251.

Saleh T.A. and Gupta V.K. (2014), Processing methods, characteristics and adsorption behavior of tire derived carbons: a review, *Advances in Colloid and Interface Science*, **211**, 93-101.

Saleh T.A. and Gupta V.K. (2011), Functionalization of tungsten oxide into MWCNT and its application for sunlight-induced degradation of rhodamine B, *Journal of Colloid and Interface Science*, **362**(2), 337-344.

Saravanan R., Sacari E., Gracia F., Khan M.M., Mosquera E. and Gupta V.K. (2016), Conducting PANI stimulated ZnO system for visible light photocatalytic degradation of coloured dyes, *Journal of Molecular Liquids*, **221**, 1029-1033.

Saravanan R., Khan M.M., Gupta V.K., Mosquera E., Gracia F., Narayanan V. and Stephen A. (2015a), $ZnO/Ag/Mn_2O_3$ nanocomposite for visible light-induced industrial textile effluent degradation, uric acid and ascorbic acid sensing and antimicrobial activity, *RSC Advances*, **5**(44), 34645-34651.

Saravanan R., Karthikeyan S., Gupta V.K., Sekaran G., Narayanan V. and Stephen A. (2013a), Enhanced photocatalytic activity of ZnO/CuO nanocomposite for the degradation of textile dye on visible light illumination, *Materials Science and Engineering: C*, **33**(1), 91-98.

Saravanan R., Joicy S., Gupta V.K., Narayanan V. and Stephen A. (2013b), Visible light induced degradation of methylene blue using CeO_2/V_2O_5 and CeO_2/CuO catalysts, *Materials Science and Engineering: C*, **33**(8), 4725-4731.

Saravanan R., Thirumal E., Gupta V.K., Narayanan V. and Stephen A. (2013c), The photocatalytic activity of ZnO prepared by simple thermal decomposition method at various temperatures, *Journal of Molecular Liquids*, **177**, 394-401.

Saravanan R., Gupta V.K., Prakash T., Narayanan V. and Stephen A. (2013d), Synthesis, characterization and photocatalytic activity of novel Hg doped ZnO nanorods prepared by thermal decomposition method, *Journal of Molecular Liquids*, **178**, 88-93.

Saravanan R., Khan M.M., Gupta V.K., Mosquera E., Gracia F., Narayanan V. and Stephen A. (2015b), ZnO/Ag/CdO nanocomposite for visible light-induced photocatalytic degradation of industrial textile effluents, *Journal of Colloid and Interface Science*, **452**, 126-133.

Saravanan R., Karthikeyan N., Gupta V.K., Thirumal E., Thangadurai P., Narayanan V. and Stephen A. (2013e). ZnO/Ag nanocomposite: an efficient catalyst for degradation studies of textile effluents under visible light. *Materials Science and Engineering: C*, **33**(4), 223.

Shifu C., Sujuan Z., Wei L. and Wei Z. (2008), Preparation and activity evaluation of p–n junction photocatalyst NiO/TiO_2, *Journal of Hazardous Materials*, **155**, 320-326.

Sohrabnezhad S., Zanjanchi M.A. and Razavi M. (2014), Plasmon-assisted degradation of methylene blue with Ag/AgCl/montmorillonite nanocomposite under visible light, *Spectrochimica Acta Part A: Molecular and Biomolecular Spectroscopy,* **130**, 129-135.

Shang M., Wang W., Sun S., Ren J., Zhou L. and Zhang L. (2009), Efficient visible light-induced photocatalytic degradation of contaminant by spindle-like PANI/$BiVO_4$, *The Journal of Physical Chemistry C*, **113**, 20228-20233.

Tonda S., Kumar S. and Shanker V. (2015), In situ growth strategy for highly efficient $Ag_2CO_3/g\text{-}C_3N_4$ hetero/nanojunctions with enhanced photocatalytic activity under sunlight irradiation, *Journal of Environmental Chemical Engineering*, **3**, 852-861.

Vadivelan V. and Kumar K.V. (2005), Equilibrium, kinetics, mechanism, and process design for the sorption of

methylene blue onto rice husk, *Journal of Colloid and Interface Science*, **286**, 90-100.

Wang S., Li D., Sun C., Yang S., Guan Y. and He H. (2014a), Synthesis and characterization of g-C_3N_4/Ag_3VO_4 composites with significantly enhanced visible-light photocatalytic activity for triphenylmethane dye degradation, *Applied Catalysis B: Environmental*, **144**, 885-892.

Wang F., Min S., Han Y. and Feng L. (2010), Visible-light-induced photocatalytic degradation of methylene blue with polyaniline-sensitized TiO_2 composite photocatalysts, *Superlattices and Microstructures*, **48**, 170-180.

Wang S., Li D., Sun C., Yang S., Guan Y. and He H. (2014b), Highly efficient photocatalytic treatment of dye wastewater via visible-light-driven AgBr–Ag_3PO_4/MWCNTs, *Journal of Molecular Catalysis A: Chemical*, **383**, 128-136.

Wang S. and Zhu Z.H. (2006), Characterisation and environmental application of an Australian natural zeolite for basic dye removal from aqueous solution, *Journal of Hazardous Materials*, **136**(3), 946-952.

Xiong P., Wang L., Sun X., Xu B. and Wang X. (2013), Ternary titania–cobalt ferrite–polyaniline nanocomposite: a magnetically recyclable hybrid for adsorption and photodegradation of dyes under visible light, *Industrial & Engineering Chemistry Research*, **52**, 10105-10113.

Xu C., Liu Y., Huang B., Li H., Qin X., Zhang X. and Dai Y. (2011), Preparation, characterization, and photocatalytic properties of silver carbonate, *Applied Surface Science*, **257**, 8732-8736.

Xu H., Zhu J., Song Y., Zhu T., Zhao W., Song Y. and Li H. (2015), Fabrication of AgX-loaded Ag_2CO_3 (X = Cl, I) composites and their efficient visible-light-driven photocatalytic activity, *Journal of Alloys and Compounds*, **622**, 347-357.

Yao T., Guo S., Zeng C., Wang C. and Zhang L. (2015), Investigation on efficient adsorption of cationic dyes on porous magnetic polyacrylamide microspheres, *Journal of Hazardous Materials*, **292**, 90-97.

Yao X. and Liu X. (2014), One-pot synthesis of ternary Ag_2CO_3/Ag/AgCl photocatalyst in natural geothermal water with enhanced photocatalytic activity under visible light irradiation, *Journal of Hazardous Materials*, **280**, 260-268.

Yu C., Wei L., Chen J., Xie Y., Zhou W. and Fan Q. (2014), Enhancing the photocatalytic performance of commercial TiO2 crystals by coupling with trace narrow-band-gap Ag_2CO_3, *Industrial & Engineering Chemistry Research*, **53**, 5759-5766.

Yu C., Zhou W., Liu H., Liu Y. and Dionysiou D.D. (2016), Design and fabrication of microsphere photocatalysts for environmental purification and energy conversion, *Chemical Engineering Journal*, **287**, 117-129.

Yao Y., Xu F., Chen M., Xu Z. and Zhu Z. (2010), Adsorption behavior of methylene blue on carbon nanotubes, *Bioresource Technology*, **101**, 3040-3046.

Yan X., Zhu X., Li R. and Chen W. (2016), Au/BiOCl heterojunction within mesoporous silica shell as stable plasmonic photocatalyst for efficient organic pollutants decomposition under visible light, *Journal of Hazardous Materials*, **303**, 1-9.

Zhang K., Wang J., Wang Y., Zhao L. and Xu Q. (2014), Facile high-yield synthesis of poly (aniline-co-m-sulfophenylenediamine) for cationic dye removal, *Chemical Engineering Journal*, **247**, 50-58.

Zheng Y., Wang W., Huang D. and Wang A. (2012), Kapok fiber oriented-polyaniline nanofibers for efficient Cr (VI) removal, *Chemical Engineering Journal*, **191**, 154-161.

Zheng J., Cheng C., Fang W.J., Chen C., Yan R.W., Huai H.X. and Wang C.C. (2014), Surfactant-free synthesis of a Fe_3O_4@ ZIF-8 core–shell heterostructure for adsorption of methylene blue, *CrystEngComm*, **16**(19), 3960-3964.

Zhao X., Lv L., Pan B., Zhang W., Zhang S. and Zhang Q. (2011), Polymer-supported nanocomposites for environmental application: a review, *Chemical Engineering Journal*, **170**, 381-394.